A guideline for pile driving fatigue assessment of welded joints and its application to offshore monopile installation

M. Orlando, J.M. van Wijk

IQIP, Molendijk 94, Sliedrecht 3361 EP, the Netherlands

Offshore wind energy has seen significant growth in recent years, driving the need for efficient and reliable foundation solutions, such as monopiles. Monopile foundations are commonly installed by means of impact pile driving. To ensure the structural integrity of the monopile foundations, which have a welded layout, correct evaluation of the cumulative fatigue damage due to the installation is essential. Currently, there is no recommended practice for modelling pile driving actions and evaluating the cumulative fatigue damage in the monopile due to impact driving. In this paper, three calculation methods with increasing complexity are presented as proposed guidelines for the engineers that will analyse this highly dynamic load case. The importance of such analysis is presented by a case study that highlights the effects of pile driving fatigue on the overall lifetime assessment of a monopile foundation. Finally, the study highlights the importance of incorporating accurate driveability predictions and realistic energy spectra for future lifetime extension calculations of a specific foundation.

Key words: Fatigue, pile driving, welded joints, stress wave analysis, monopile, finite element method

1 Introduction

Over the past decade the wind energy sector has experienced a substantial growth, leading to an increase in global demand for wind turbines from 125 GW in 2023 to the forecasted scenarios of 170 GW in 2035 and 206 GW in 2050 [IEA, 2024]. In order to achieve these challenging targets, efficient and reliable offshore support structures are needed, such as monopiles, jackets or tripods. Despite the heavier weight, currently monopiles represent the simplest and most effective design layout for offshore wind turbine foundations compared to the other foundation types [Moulas et al., 2017]. The general design layout of a monopile can be described as a series of longitudinally welded pipes, with both cylindrical and conical sections, welded together by butt welds to achieve the desired foundation length.

Offshore monopile installation is predominantly executed by means of impact hammers, that generate high dynamic forces for each blow [Jiang, 2021; Meijers et al., 2018]. The stress waves introduced by each impact locally compress the pile, and the waves travel through the pile to reach the pile tip. Energy is dissipated by means of shaft resistance and ultimately displacement of the soil around the pile tip. The repeated application of high impact loading causes cumulation of fatigue damage, resulting in a reduction of the foundation in-service lifetime.

Fatigue accumulation during the in-service period of the foundation receives much attention, as the larger part of damage is accumulated over this period due to the operational and environmental loads [Mehmanparast et al., 2017; Biswal and Mehmanparast, 2019; Velarde et al., 2020].

The installation-accumulated fatigue damage makes for a smaller, but still significant portion of the overall accumulated fatigue damage, and as such is relevant for optimization of the foundation and installation method.

After pile installation, the accumulated fatigue damage can be precisely analysed based on the driving records, namely the overview of every individual impact and their associated energy levels for a specific hammer-pile combination, as described by Orlando [Orlando et al., 2023].

A fatigue assessment prior to installation however requires a different approach, which primarily can be based on Finite Element (FE) modelling [Orlando et al., 2021; Hu et al., 2023]. Despite the availability of advanced computational tools, no standard approach for installation fatigue assessment exists in the industry, and some studies have been presented over the past years, heavily relying on simplified 1D numerical analyses based on stress waves equations [Chung et al., 2013, Ozsu et al., 2013]. In this paper three methods based on validated detailed FE models are presented to provide guidelines for the correct evaluation of the cumulative fatigue damage of welded joints subjected to pile driving. After a brief description of the pile driving operations, the fatigue assessment framework is presented and then adopted for a case study to demonstrate its application, also accounting for actual driving records. Finally, potential improvements to the current methodology are presented as basis for future work that will improve the assessment of welded joints under pile driving loads.

2 Pile driving overview

The equipment needed to install offshore monopile foundations is presented in Figure 1, where a hydraulic impact hammer and sleeve are shown standing on top of a monopile.

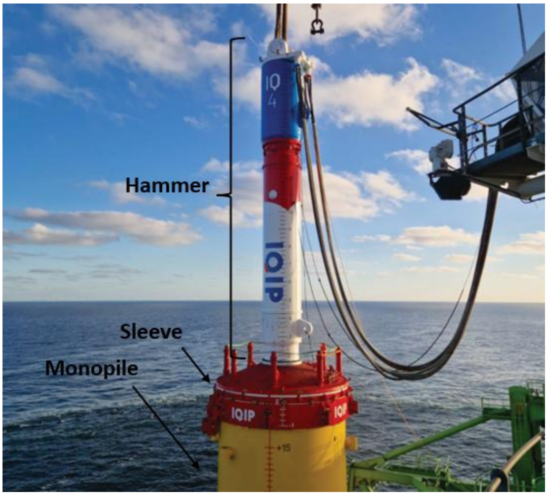

Figure 1. Hydraulic impact hammer, sleeve and monopile

The impact hammer is a hydraulically operated machine in which a steel ram is lifted by the hydraulics up to an upper dead point and then accelerated downward to hit on the anvil, a loose plate placed inside the sleeve, which transfers the impact energy to the monopile top as a stress wave (or force wave). During installation, the hammer assembly is supported on the monopile sideways by the sleeve, that can have different lengths based on the different hammer and pile configurations. A cutaway view of a standard hammer sleeve configuration installed on a monopile is shown in Figure 2.

At the moment of impact between the anvil and the monopile, a compressive stress wave is generated at the top of the pile which then travels down along its axis. While travelling down the pile, the magnitude of the stress wave reduces due to the friction between the pile and the soil and when a change in impedance occurs the stress wave is reflected and it moves upward again. Stress wave reflection can occur at a section transition or at the pile tip. The sign of the reflected stress wave at the pile tip is determined by the boundary conditions at this location, and it occurs that in case of a penetrating pile the reflected wave is a tensile wave, while in case of pile at refusal the returning stress wave is reflected as a compressive wave.

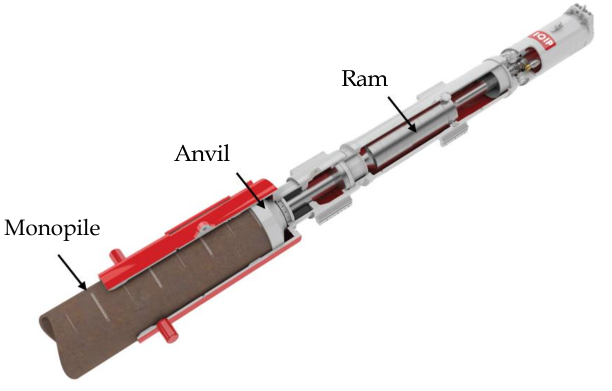

Figure 2. Hammer, sleeve and monopile cutaway view

The simulations of the stress wave propagation in the monopile and the interaction between monopile and soil during impact are performed with well-known driveability software based on 1D stress wave equation solvers [Smith, 1960; Middendorp et al., 2006]. These methods are still the common tool in geotechnical engineering practice for pile driveability assessments, that focus on the pile-soil interaction.

Figure 3 shows results from 1D simulations in case of a penetrating pile, where plots over time of the longitudinal force in a cylindrical monopile during a blow are presented. In particular, results over time at three different pile locations are plotted, namely the top of the monopile (blue curve), the mid-section of the monopile (red curve) and the tip of the monopile (yellow curve). It must be noted that, consistently with the notation adopted in geotechnical analysis, in the figure compression is reported as positive. The compressive stress wave starts at the pile top and it peaks at this location between 141 s and 141.01 s, then it starts rising in the mid-section, where it peaks between 141.01 s and 141.02. Finally, the compressive wave reaches the pile tip as shown by the rising yellow curve, and it is reflected in form of a tensile wave, i.e. with negative sign, towards the pile mid-section, where it peaks between 141.03 s and 141.04 s.

In Figure 4 results from the 1D simulation are reported with same colours and notation for a pile at refusal. In this case the initial compressive stress wave starting at the pile top, reaches the pile tip around 1005.02 s, and from there it is reflected as a compressive wave towards the pile mid-section, shown by the positive sign of the red curve around 1005.03 s.

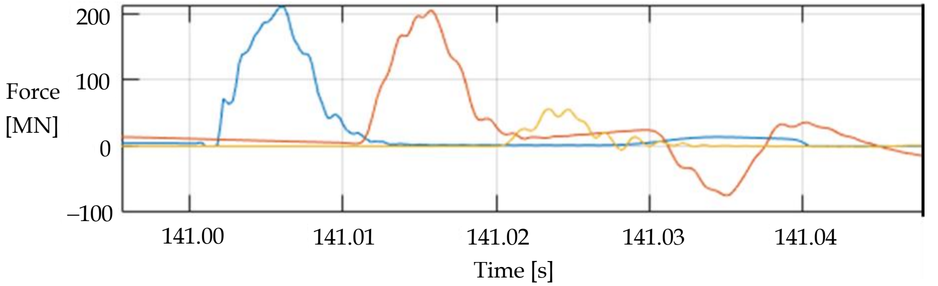

Figure 3. Simulation of penetrating pile – Force at the pile top (blue), force in the pile mid-section (red) and force in the pile tip (yellow), compression is positive

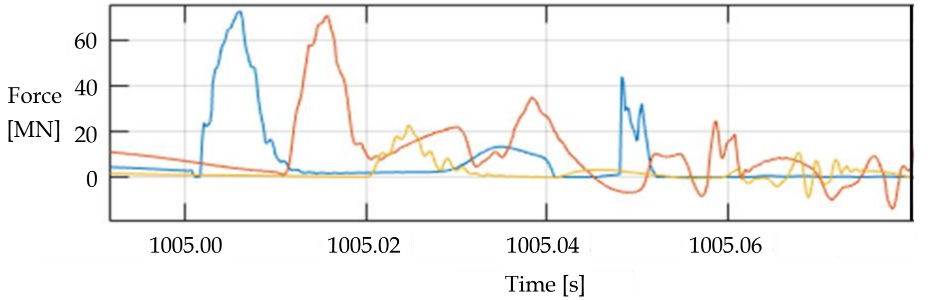

Figure 4. Simulation of pile at refusal – Force at the pile top (blue), force in the pile mid-section (red) and force in the pile tip (yellow), compression is positive

Results accuracy of the 1D simulations adopted for geotechnical investigations, can be improved by including more advanced anvil models based on reduced order modelling and FEA, especially for monopiles with diameters larger than 5.5 m [Ligthart et al. 2022]. Although commercially available 1D stress wave equation solvers for pile driveability produce stress maxima results in the spatio-temporal domain, these methods are insufficient for large diameter piles due to the complex nature of stress wave propagation in these foundation types that include vibrations and bending at the pile top. These modelling limitations can cause underestimation of the fatigue actions at the monopile top resulting in non-conservative fatigue damage calculations.

3 Fatigue assessment of welded connections subjected to pile driving actions

Fatigue is a critical failure mode for welded joints, and it is estimated that 80% to 90% of failures in steel structures are due to fatigue [FADLESS, 2014]. As a result, it is essential to have reliable assessment techniques to prevent unforeseen failures and enhance structural safety, while also optimizing steel usage in construction to reduce production costs.
As outlined by Orlando [Orlando et al., 2023], pile driving fatigue assessments are typically carried out during the preliminary design phase of monopile foundations, using methods such as one-dimensional models and wave equation analysis that consider the effects of soil-pile interaction. A common result from these simplified analyses is the longitudinal stress ranges at each section of the pile, which are then used in a stress-based fatigue calculation based on the *S-N* curves from relevant standards, such as the DNV-RP-C203 [DNV, 2024] recommended practice.

However, as explained in the previous chapter, these one-dimensional models are limited in their ability to account for the local bending and vibration effects at the top of the monopile, which can be significant, especially for larger piles. In addition to this, in cases where complex connections exist between the monopile and transition piece or tower, such as bolted flanges or novel connection types, advanced FE modelling is required to accurately calculate local stresses.

In the next sections, three different calculation methods, based on FE methodology validated against experimental measurements [Orlando et al., 2022], are briefly presented to propose guidelines to follow based on the modelling requirements.

3.1 ***Calculation method 1***

The simplest calculation method, here presented as calculation method 1, is based on the assumptions of components with perfectly *symmetric geometries* and *ideal impact surfaces*. This is the case on preliminary design calculations where (butt) welded joints exist between each can of the analysed monopile. Under these assumptions, the methodology for the fatigue calculation of welded joints can be executed as follows:

- Fatigue stress cycles to be evaluated from the execution of implicit 2D axisymmetric dynamic simulations with a simulation time of ~100 msec.
- 2D axisymmetric linear elements are used to model the components.
- Modelling of non-linear contact between the components that allow separation (i.e. the inability to transfer a tensile stress wave) when subjected to a "tensile" force at the interface.
- Pile tip is free to move, i.e. not constrained in the longitudinal direction to be representative of a penetrating pile. This boundary condition guarantees a tensile reflected stress wave at the pile tip.
- The stress wave amplitude of the returning waves is affected by energy dissipation at the pile-soil interface, and should be included in the analysis. Pile-soil interaction direct modelling in FE can be neglected, but will be included by post-processing of FEA results using the results of a driveability analysis performed with 1D wave equation models. These calculations are performed by accounting for the specific soil conditions and driving procedures using the hammer, anvil and sleeve configuration also used in FEA. This implies that a total number of P 1D stress wave analyses are conducted, on a pile discretized in M segments, driven over N depth intervals in the soil.

Once these calculations are completed, a scaling factor f_s can be calculated as the ratio between the reflected tensile σ_t stress wave and the compressive stress wave σ_c for each pile segment i, penetration level j and energy level k as:

$$f_s[i,j,k] = \left(\frac{\sigma_t}{\sigma_c}\right)_{i,j,k} \tag{1}$$

Then, averaging each scaling factor over each of the M pile segments gives the length-averaged scale factor:

$$\bar{f}_s[j,k] = \frac{1}{M}\sum_{i=1}^{M} f_s[i,j,k] \tag{2}$$

To include the actual number of load cycles over the pile installation sequence, the length-averaged scale factor will be averaged over the blow count B (which is a result of the 1D driveability analysis: at each depth interval j out of the N depth intervals in total, a number energy level k as:

$$\bar{f}_s[k] = \frac{\sum_{j=1}^{N[k]} \bar{f}_s[j,k]\, B[j,k]}{\sum_{j=1}^{N[k]} B[j,k]} \tag{3}$$

Finally, the equivalent scaling factor can be found by averaging over the P energy levels, resulting in:

$$f_{eq} = \frac{1}{P}\sum_{k=1}^{P} \bar{f}_s[k] \tag{4}$$

Stress signal in time can be scaled by the equivalent scaling factor only for the part related to the reflected stress wave to generate updated "scaled" stress signals for fatigue evaluation. In Figure 5 examples of both the stress signal from the original FE calculation and the scaled stress signal are reported to show the effects of scaling due to pile/soil interaction on the stress magnitude.

- Once the stress cycles are obtained, fatigue checks can be executed, for example, according to the rules presented in DNV-RP-C203 for the welded joints under investigation.

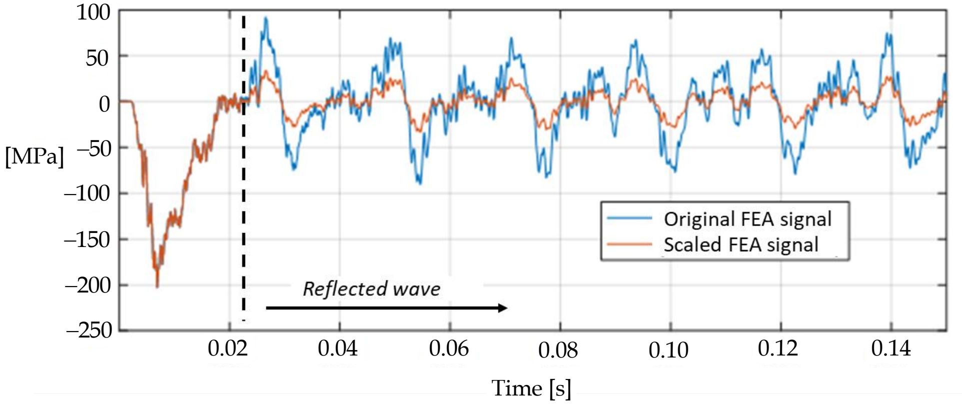

Figure 5. Longitudinal stress in the monopile top can from FEA (blue), and scaled stress for fatigue checks (orange)

3.2 ***Calculation method 2***

A more refined calculation method to be adopted in case of monopiles with *non-axisymmetric features*, such as welded trunnions, or in case inclinations and/or misalignments between impacting bodies must be included, can be described as follows:

- Fatigue stress cycles to be evaluated from the execution of implicit 3D dynamic simulations.

- 3D solid linear elements can be adopted, together with 3D solid quadratic elements in the critical regions of the model.

- The same assumptions and same scaling factors of method 1 can be adopted.

3.3 ***Calculation method 3***

When *imperfections* of the analysed geometries shall be accounted for, such as unevenness or waviness of the impact surfaces, this calculation method can be used for fatigue calculations of welded joints:

- Fatigue stress cycles to be evaluated from the execution of implicit 3D dynamic simulations as in method 2.

- Modelling of a circular sector representative of the local unevenness or waviness of the impact surfaces at the pile top assumed as a sinusoidal curve with the following approach:

  - Top pile unevenness as specified by the pile manufacturing drawing based on the "short-wave" or local values. A typical value for the local unevenness is 1 mm over 30° as per DNV-ST-0126 [DNV, 2021]. This out-of-flatness can be modelled as a smooth sinusoidal wave at the pile top, as also mentioned by Seidel [Seidel, 2018].

  - The bottom anvil (or ring anvil) out-of-flatness is typically lower than the one reported for the pile, and it can be neglected for fatigue calculation purposes since the probability of the two waviness peaks being in contact at every blow is limited.

- The same modelling assumptions of method 1 can be adopted.

4 Case study

A conical monopile with L-flange at the pile top and an air-tight platform support structure welded at the pile inner diameter is presented as a case study to demonstrate the application of Calculation Method 3. The following hammer – anvil combination is used for this study:

- IQIP S-2000 hammer, with a maximum impact energy of 2000 kJ. For the analysis, only the hammer ram is modelled.
- IQIP 5.5 m anvil.
- 5.5 m top diameter monopile with 80 mm wall thickness and a length of 66 m.

For this specific calculation, a 180° circular sector of the monopile has been modelled as shown in Figure 6.

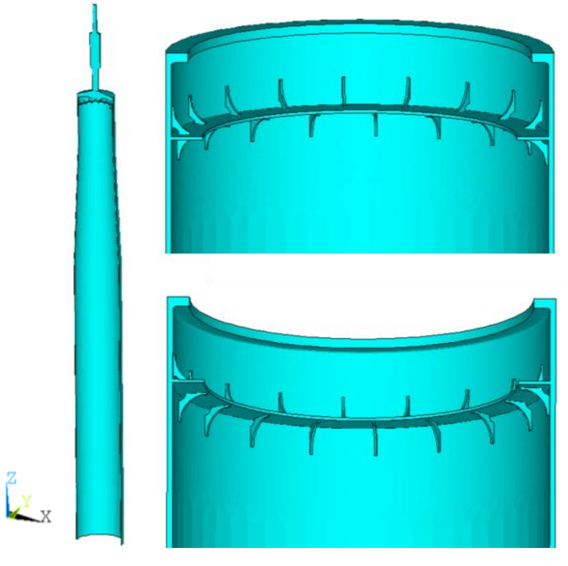

Figure 6. 5.5 m Monopile case study - Geometry of the modelled hammer ram, anvil and pile

At the monopile top, a butt-welded joint connects the L-flange to the top monopile can, and full penetration welds are connecting the air-tight platform supports to the inner surface of the monopile. In Figure 7, the air-tight platform support plates are shown and numbered. At the top of the monopile an unevenness of 1 mm over 30° has been modelled according to the curve reported in Figure 8.

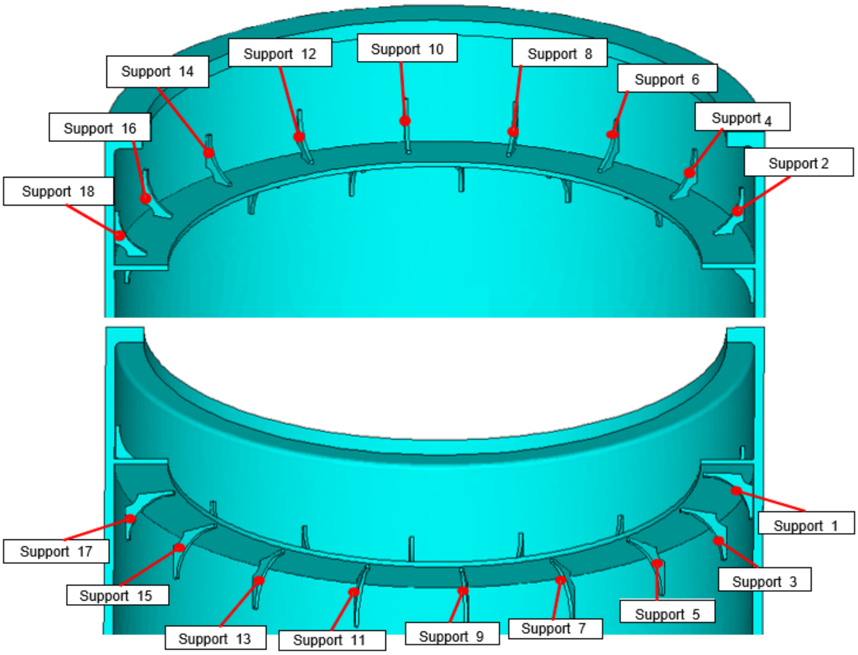

Figure 7. 5.5 m Monopile case study – Indication of air-tight support structure plates

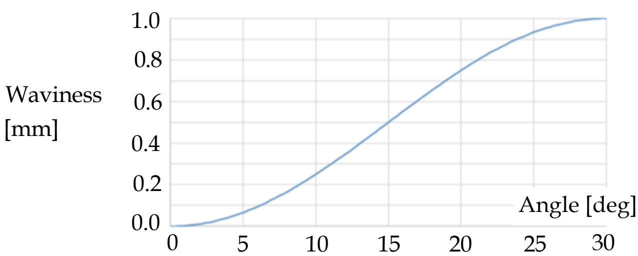

Figure 8a. 5.5 m Monopile case study – Pile top waviness curve, crest at 30°

In Figure 8b details of the mesh at the pile top are presented. 3D linear elements are generally adopted, while 3D quadratic elements are used in the region of interest at the monopile top, as also mentioned in Figure 8b.

Symmetric boundary conditions have been applied on the symmetry plane, and an initial impact velocity of 6.3 m/s is imposed on the hammer ram to achieve the maximum energy of 2000 kJ. No gravity is considered in the analysis since its contribution is negligible compared to the magnitude of the loads due to impact driving.

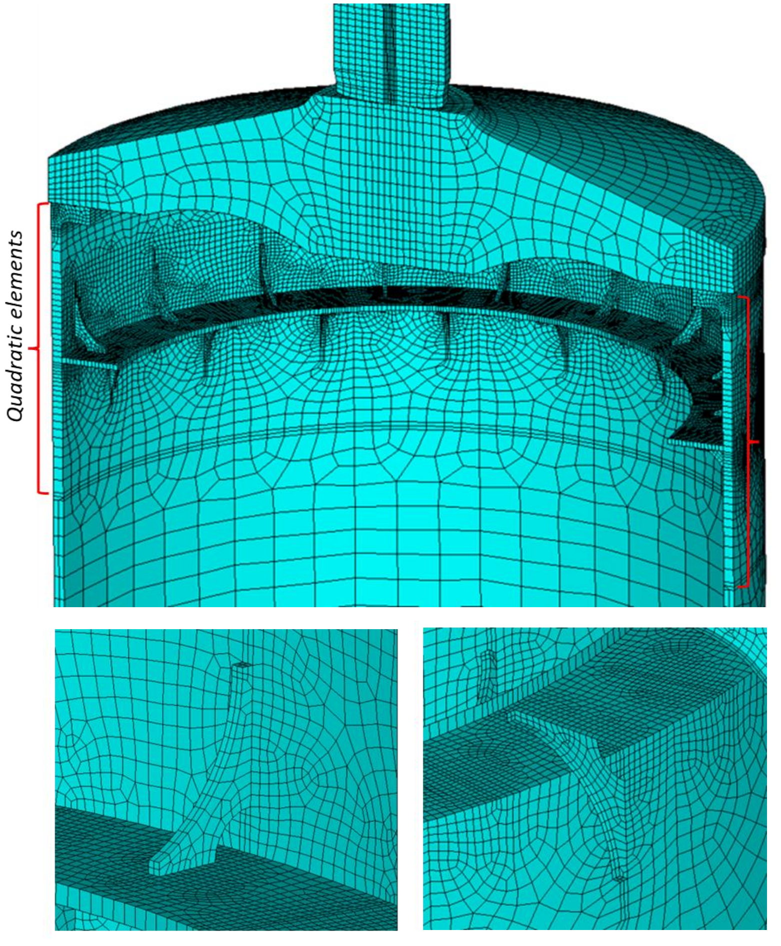

Figure 8b. 5.5 m Monopile case study – Mesh of welded details

4.1 Calculation results

A non-linear transient calculation is executed in ANSYS to extract stresses at the welded joint locations for fatigue damage evaluation in accordance with the guidelines of DNV-RP-C203. Figure 9 shows the longitudinal stresses at the inner pile section for the moment of maximum local compressive stress, with the most critical location reported in the red box. Local stress peaks at the inner side of the pile occur at the location of the waviness crest, i.e. at 30°, 90° and 120° along the circumference of the pile. In Figure 10 the longitudinal stress at the most critical support plate, Support 4 of Figure 7, is shown for the moment of maximum local stress, that occurs at the pile wall where the support tip is located.

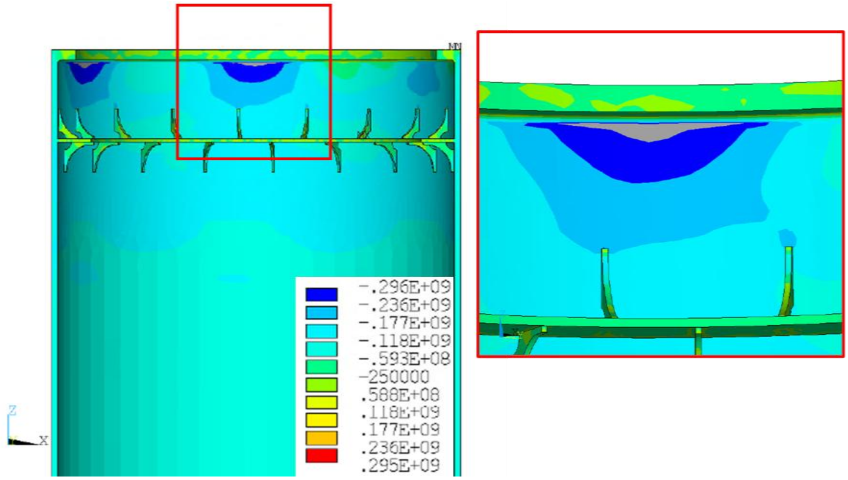

Figure 9. 5.5 m Monopile case study – Contour plot of longitudinal stress at the inner pile for the moment of maximum stress [Pa]

Based on preliminary driveability analyses with a 1D wave equation model including pile-soil interaction, an average scaling factor for the reflected (tensile) stress wave is calculated at several pile section locations as a function of multiple impact energies. In Table 1 the ratios between tensile and compressive stress wave for each location extracted from the 1D model analyses are reported, and from these values an average scaling factor of 0.55 has been applied after ca. 26 ms on the reflected tensile wave to evaluate the stress cycles for this case study.

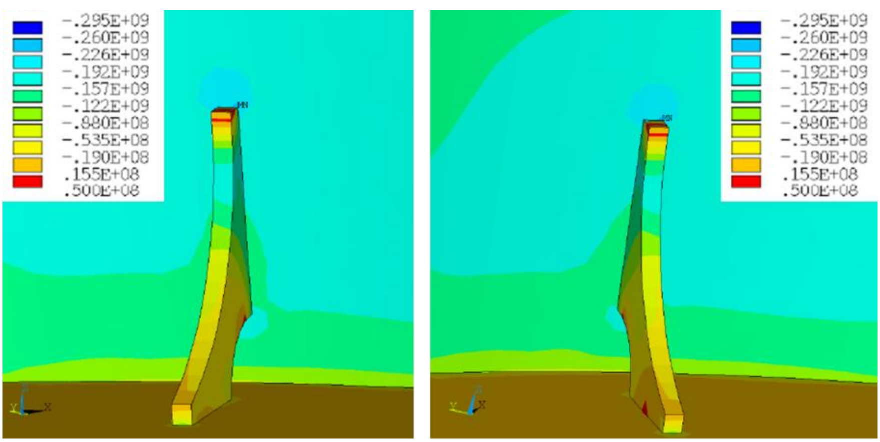

Figure 10. 5.5 m Monopile case study – Contour plot of longitudinal stress at the most critical top support plate for the moment of maximum stress [Pa]

Table 1. *Scaling factors for different impact energies at different pile section locations*

Location nr.	1	2	3	4	5	6	7	8	9	10
Rel. distance from pile top	13%	16%	26%	40%	44%	54%	71%	76%	80%	95%
Impact energy	σ_t/σ_c									
10%	0.53	0.49	0.48	0.55	0.56	0.55	0.57	0.55	0.52	0.49
25%	0.53	0.50	0.47	0.52	0.53	0.55	0.59	0.58	0.55	0.46
50%	0.53	0.50	0.46	0.53	0.54	0.56	0.61	0.60	0.57	0.41
75%	0.55	0.50	0.48	0.55	0.57	0.59	0.62	0.61	0.59	0.43
2000 kJ = 100%	0.57	0.51	0.48	0.55	0.57	0.60	0.64	0.62	0.59	0.43

The principal stress directions for the investigated welded joints are in the longitudinal direction, and plots over time of the longitudinal stress for both the worst location of the butt-weld between L-flange and monopile and the most critical top support plate are reported in Figure 11 and Figure 12 respectively. In the figures stresses from FEA and stresses scaled with average scaling factor of 0.55 as per Table 1 are reported. In particular, for the most critical top support plate, the hot spot stress is evaluated according to the DNV methodology, by linearly extrapolating the stresses evaluated at half the wall thickness and 1.5 times the wall thickness distance from the toe of the weld under investigation.

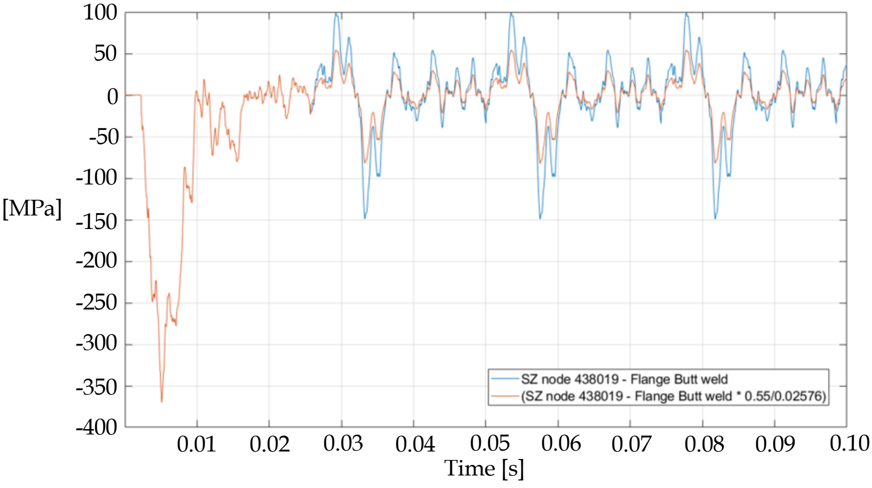

Figure 11. 5.5 m Monopile case study – Longitudinal stress (negative is compression) at the butt-weld join between L-Flange and pile as function of time, stress from FEA (blue) and scaled stress for fatigue checks (orange)

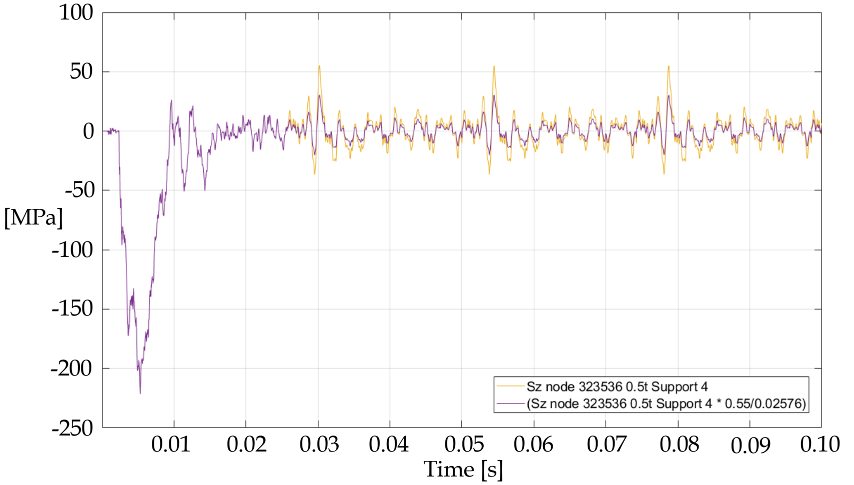

Figure 12. 5.5 m Monopile case study – Hot spot longitudinal stress (negative is compression) at the most critical support plate as function of time, stress from FEA (yellow) and scaled stress for fatigue checks (purple)

Based on the time traces of Figure 11 and 12, fatigue damage calculations have been performed based on 4000 blows at maximum impact energy, which is considered sufficient to drive the pile down to final penetration.

For the purpose of this case study, the following structural details according to DNV-RP-C203 have been assumed, not considering the effects on the mean stress reduction due to the lack of post-weld-heat-treatment for the analysed welded joints, see Figure 13:

- Butt-weld between the L-flange and the first monopile can: C1 (in air).
- Full-penetration weld between the support plate and pile: D (in air).

Finally, the cumulative fatigue damages due to pile driving after 4000 blows at maximum impact energy is assessed assuming linear damage accumulation as per Palmgren-Miner's rule. The total damage D is calculated by rainflow counting technique in accordance with ASTM E1049-85 [ASTM, 2017]. The sum of the damages of each blow d_b :

$$D = \sum_{b=1}^{n_{blow}} d_b \tag{5}$$

Detail	Figure	Category	Description	Requirements
Transverse butt weld, welded from both sides	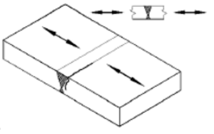	C1	Circumferential butt weld made from both sides machined or ground flush	• The applied stress shall include the stress concentration factor to allow for any thickness change and for fabrication tolerances • All welds ground flush to plate surface parallel to direction of the arrow. • Weld run-off pieces to be used and subsequently removed. • Plate edges to be ground flush in direction of stress. • All welds welded in flat position in shop.
Hot spot stress curve	N/A	D	Crack from the weld toe	• Full penetration weld

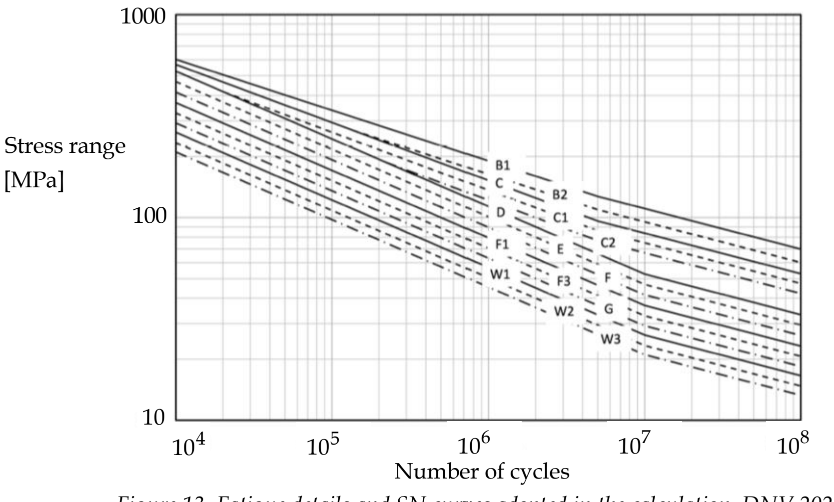

Figure 13. Fatigue details and SN curves adopted in the calculation, DNV 2024

And the damage per blow is calculated as the sum of the damages of each stress bin, that is equal to the ratio between q_c , i.e. the number of constant stress cycles in the specific bin *c*, and Q_c , i.e. the number of cycles to failure at the same constant stress range:

$$d_b = \sum_{c=1}^{n_{bin}} \frac{q_c}{Q_c} \tag{6}$$

The cumulative fatigue damages for the two welded joints under investigations are calculated based on a design fatigue factor equal to 1 as:

- Butt-weld between the L-flange and the first monopile can: 0.30.
- Full-penetration weld between the support plate and pile: 0.10.

The resulting fatigue damages are the initial cumulative damages that must be added to the in-service lifetime of the respective welded joints to establish the service lifetime of the monopile foundation.

5 Further improvements to the calculation methods

One of the main improvements to the presented methodologies can be identified as the possibility of considering a more realistic and less conservative energy spectrum when executing the stress cycle evaluation. Executing every blow at the maximum hammer rated impact energy is not realistic, and accounting for driveability predictions in which every blow is analysed with the expected impact energy for each penetration depth in best estimate or upper bound soil conditions can lead to a reduction up to 63% in calculated fatigue damage [Orlando et al., 2023]. This reduction in fatigue damage can also increase dramatically in case the actual installation will be finalised with lower impact energies and a smaller number of blows compared to the initial driveability predictions.

However, it is not advised to adopt this less conservative approach in the design stage of the monopile as uncertain soil conditions are difficult to be accounted for. There is, however, potential in using these less conservative methods when assessing the remaining fatigue life of a foundation for lifetime extension of offshore wind turbines, i.e. a post-installation assessment.

6 Conclusions

Fatigue damage accumulation during the in-service period of foundation is an active area of research, however the damage accumulation during foundation installation is informed mainly by industry practice without the existence of general guidelines.

This paper has presented a comprehensive methodology for assessing the cumulative fatigue damage of welded joints in offshore monopile foundations subjected to impact pile driving that overcomes the overly simplified assumptions currently in literature that are based on 1D numerical models.

The proposed methodology consists of a combination of finite element analysis and 1D stress wave analysis. The FEA is used for assessing the actual loading on the top of the monopile, while the 1D stress wave analysis is used to determine a correction factor on the stress amplitude of the reflected waves. This correction which is a novel way of post-processing FEA for fatigue analysis, is required to include the energy dissipation through the pile-soil interaction, and the method presented in this paper is valid for different levels of sophistication in FEA.

The case study presented in this paper demonstrates how the methodology can be applied to fatigue assessment of welded joints in offshore monopiles. Finally, it is discussed how incorporating actual driving records can lead to a more accurate and less conservative estimation of fatigue damage compared to traditional design-stage assumptions, which typically could be part of a post-installation fatigue damage assessment.

Literature

ASTM. ASTM E1049-85(2017). Standard Practices for Cycle Counting in Fatigue Analysis, 2017. Available online: https://store.astm.org/e1049-85r17.html

Biswal, R., Mehmanparast, A., Fatigue damage analysis of offshore wind turbine monopile weldments, *Procedia Structural Integrity* 17 (2019) 643–650, 2019.

Chung, J., Wallerand, R., Hélias-Brault, M. Pile fatigue assessment during driving, *Procedia Engineering* 66 (2013) 451 – 463, 2013.

DNV. DNV-RP-C203. Fatigue of offshore steel structures, 2024. Available online: https://www.dnvgl.com/

DNV. DNV-ST-0126. Support structures for wind turbines, 2021. Available online: https://www.dnvgl.com/

FADLESS. Fatigue damage control and assessment for railway bridges (FADLESS). Final report, 2014. Available online: https://op.europa.eu/en/publication-detail/-/publication/e5a5a775-2b64-4d58-b714-a10eee3dae45

Hu, H., Yan, Y., Feng, X., Cao, C., Mei, W., Jiang, Q., Sun, B., Ni, Z. Fatigue analysis of large anvil in the pile driving of offshore wind turbines, *Ocean Engineering* 283 (2023) 115017, 2023.

IEA. Energy Technology Perspective 2024, IEA, Paris, 2024. Available online: https://www.iea.org/reports/energy-technology-perspectives-2024

Jiang, Z. Installation of offshore wind turbines: A technical review, *Renewable and Sustainable Energy Reviews* 139 (2021) 110576, 2021.

Ligthart, J. and Orlando, M. A novel anvil modelling approach for pile driveability prediction, 2022. Presented at the *SW2022 Conference*. Available online: https://community.kivi.nl/paper/a-novel-anvil-modelling-approach-for-pile-driveability-prediction-validated-with-pda-measurements

Mehmanparast, A., Brennan, F., Tavares, I. Fatigue crack growth rates for offshore wind monopile weldments in air and seawater: SLIC inter-laboratory test results, *Materials and Design* 114 (2017) 494–504, 2017.

Meijers, P. C., Tsouvalas, A., Mitrikine, A. V. A non-collocated method to quantify plastic deformation caused by impact pile driving, *International Journal of Mechanical Sciences* 148 (2018) 1–8, 2018.

Middendorp, P. and Verbeek, G.E.H. 30 Years of Experience with the Wave Equation Solution Based on the Method of Characteristics. *GeoCongress 2006*, 2006.

Moulas, D., Shafiee, M. and Mehmanparast, A. Damage Analysis of Ship Collisions with Offshore Wind Turbine Foundations. *Ocean Engineering*, Volume 143, Pages 149-162, 2017.

Orlando, M., Ligthart, J., van Wijk, J., Raymackers, S. PDA measurements: fact or fiction, 2022. Presented at the *SW2022 Conference*. Available online: https://community.kivi.nl/wp-content/uploads/SW2022Orlando.pdf

Orlando, M., Ligthart, J., van Wijk, J., Schaap, M. Pile installation fatigue damage from impact driving records – A case study of offshore monopiles, 2023. Presented at the 1st *Annual Conference on Foundation Decarbonization and Re-use*. Available online: https:// https://foundationreuse.com/wp-content/uploads/2023/07/Foundation-Reuse-Orlando.pdf

Ozsu, E., Ta, A., Stuyts, B., Jaeck, C. Optimizing Pile Driving Fatigue for Offshore Foundations in Very Dense Sand: A Case Study (Draft), Proceedings of the ASME 2013 32nd *International Conference on Ocean, Offshore and Arctic Engineering*, 2013.

Seidel, M. Tolerance requirements for flange connections in wind turbine support structures, Stahlbau, 87: 880-887, 2018.

Smith, E.A.L. Pile Driving Analysis by the Wave Equation, *ASCE Journal of the Soil Mechanics and Foundation Division*, 86(4), 35–61, 1960.

Velarde, J., Kramhøft, C., Sørensen, J. D., Zorzi, G. Fatigue reliability of large monopiles for offshore wind turbines, *International Journal of Fatigue*, 134, Article 105487, 2020.